Quantum Electronics **49** (7) 633–640 (2019)

https://doi.org/10.1070/QEL16890

Absolute frequency measurements for emission transitions of molecular iodine in the range of 1053–1068 nm

M.I. Nesterenko, S.M. Ignatovich, S.A. Kuznetsov, Yu.A. Matyugin, M.N. Skvortsov

Abstract. **Results of high-precision frequency measurements are presented for certain components of the $^{127}I_2$ hyperfine structure, which correspond to emission transitions of the B–X band in the range of 1053–1068 nm. The frequencies are measured by using a femtosecond optical frequency synthesiser based on a Ti:sapphire laser. The hyperfine structure is resolved by the method of three-level laser spectroscopy. The frequency-doubled cw Nd:YAG laser is used as an excitation radiation source, and the probe radiation in the range of 1050–1070 nm is generated by an external-cavity diode laser. The frequencies of both lasers are simultaneously locked to those of two adjacent hyperfine structure components of iodine lines, which have a common upper level. Correspondingly, the frequency of the Nd:YAG laser is locked to the frequency of the absorption transition component, and the diode laser frequency – to the frequency of the emission transition component. The radiation frequency of the diode laser 'locked' in this way is measured. Frequencies of 18 hyperfine structure components for six emission lines corresponding to the bands (32–54) and (32–53) are measured. The relative uncertainty of the measurement is 8×10^{-10}.**

Keywords: *spectroscopy of molecular iodine, three-level laser spectroscopy, Nd:YAG laser, external-cavity diode laser, femtosecond optical frequency synthesiser, optical frequency measurement.*

1. Introduction

Presently, frequencies of several hundred transitions in iodine molecule have been measured with high accuracy. All the measurements have been taken for the absorption spectrum of the B–X system mainly in ranges of 526–667 nm and 750–815 nm. A detailed bibliography on this theme (up to 2010) is given in [1–7]. Analysis of the entire scope of high-precision results performed in [2] showed that the transitions studied include vibration levels of the B state with quantum numbers $v' \leqslant 43$ and of the X state with quantum numbers v'' in the limits $0 \leqslant v'' \leqslant 7$ and $12 \leqslant v'' \leqslant 17$. Results of these measurements more precisely specified energies of these vibration levels and a shape of the potential curve for the B state, and, finally, provided improved data on iodine spectroscopic parameters for the B–X band. In turn, these parameters make it possible to calculate the frequencies of arbitrary absorption transitions of the B–X band with high accuracy. In view of this fact, the iodine absorption spectrum may serve as a frequency scale for calibrating laser frequencies with an accuracy no worse than 10^{-9}. In recent years, high-precision measurements were taken for a series of iodine absorption transitions in the range of 548–671 nm [8–12].

Data obtained are not sufficient for constructing a more precise potential curve for the fundamental electron X state, and additional data cannot be obtained from measurements of absorption transition frequencies, because only a few of lowest thermally populated vibration–rotational levels of the X state participate in forming the absorption spectrum. The required data for the fundamental electron state can be obtained only by measuring frequencies of emission transitions, because an emission spectrum is formed due to transitions from an excited electron level of the B state to any level of the X state.

Presently, a potential curve for the X state is constructed basing on the data obtained from frequency measurements of the Doppler-broadened emission lines with unresolved hyperfine structure [13]. The accuracy of such measurements performed with a Fourier spectrometer is 2×10^{-7}.

We have demonstrated a possibility of high-precision frequency measurements for emission transitions in 2008 and 2012 (see, [5, 7]). For obtaining narrow optical resonances corresponding to hyperfine structure (HFS) emission lines we used the method of three-level laser spectroscopy [14]. For obtaining emission resonances with the frequency exactly equal to the emission transition frequency we used the method based on simultaneous locking the radiation frequencies of two lasers to the frequencies of two adjacent transitions with a common upper level. In this case, one of the transitions is absorption transition and the other is emission. For the absorption transition, the optical resonance is obtained by the saturation absorption method, and for the emission transition, it is the three-level laser spectroscopy. The laser with the frequency locked to the absorption resonance frequency serves as a pump laser in the three-level spectroscopy method. A single-frequency radiation of this laser excites to the upper level only those molecules, which have a close-to-zero velocity projection to the laser beam axis. As a result, the narrow optical resonance arises in the spectrum of emission transition, whose centre coincides exactly with the transition frequency. Such a resonance can be used as a frequency reference for stabilising laser frequencies, and, correspondingly, for measuring radiation frequencies of an emission transition.

By using the method suggested and a femtosecond frequency synthesiser, we for the first time measured the fre-

M.I. Nesterenko, S.M. Ignatovich, S.A. Kuznetsov, Yu.A. Matyugin, M.N. Skvortsov Institute of Laser Physics, Siberian Branch, Russian Academy of Sciences, prosp. Akad. Lavrent'eva 15B, 630090 Novosibirsk, Russia; e-mail: maxnest@gmail.com

Received 30 October 2018
Kvantovaya Elektronika **49** (7) 633–640 (2019)
Translated by N.A. Raspopov

quencies of 20 HFS emission components in the range of 982–985 nm with a relative error of 7×10^{-10} [7]. Similar high-precision measurements taken in the whole range of the iodine emission spectrum will form a database for constructing a more accurate potential curve of the fundamental electron state of the iodine molecule and will provide more accurate spectroscopic parameters used for calculating emission transition frequencies. As a result, the emission spectrum may serve as a frequency scale for high-precision calibration of laser radiation in the range of 500–1340 nm.

In this work, we present high-precision measurement results for the HFS components of $^{127}I_2$ molecule emission lines in the range of 1053–1068 nm corresponding to the (32–53) and (32–54) bands of the B–X system.

2. Experimental setup

The experimental setup comprises a laser spectrometer, which provides locking the frequency of a diode lade laser to the frequency of an iodine emission transition, and a measuring complex based on a femtosecond optical frequency synthesiser. The complex provides absolute frequency measurements of diode laser radiation and studying frequency characteristics of the laser.

The laser spectrometer is a combination of two spectrometers: the saturated absorption spectrometer and three-level spectrometer. The former provides frequency locking to the absorption transition frequency, and the latter locks the sounding laser frequency to the emission transition frequency. The setup is described in more details in [5, 7]. Minor changes were made in the setup while conducting the present work.

A principal schematic of the spectrometer is shown in Fig. 1. A frequency-doubled cw Nd:YAG laser is used as pump radiation in the spectrometer. Probing of the emission transition is realised with radiation of an external-cavity diode laser. Radiation beams of both the lasers coincide in a cell with iodine vapours.

In the present work we employ a diode-pumped Nd:YAG laser with an intracavity frequency doubler developed at the Institute of Laser Physics, Siberian Branch of RAS (Novosibirsk) [15]. The laser has a ring non-planar cavity, which provides a single-frequency operation with a unidirectional running wave. The cavity has temperature stabilisation and a rigid construction, which provides a narrow (at most 10 kHz) laser emission line in the free operation regime. The range of laser radiation frequency tuning is 300 GHz (1064.0–1065.3 nm), so that the second harmonic is tuned in the range of 532.6–532.0 nm. The output power of the second harmonic radiation at the centre of the tuning range is ~7 mW and falls twice in wings.

The sounding radiation source was a tunable external-cavity diode laser based on an autocollimation scheme with a V-type configuration similar to that used earlier in [16]. The beam collimated by a micro-objective passes to a semitransparent mirror, which directs it at a required diffraction angle to the grating (1800 lines mm^{-1}) arranged on a piezoceramic actuator.

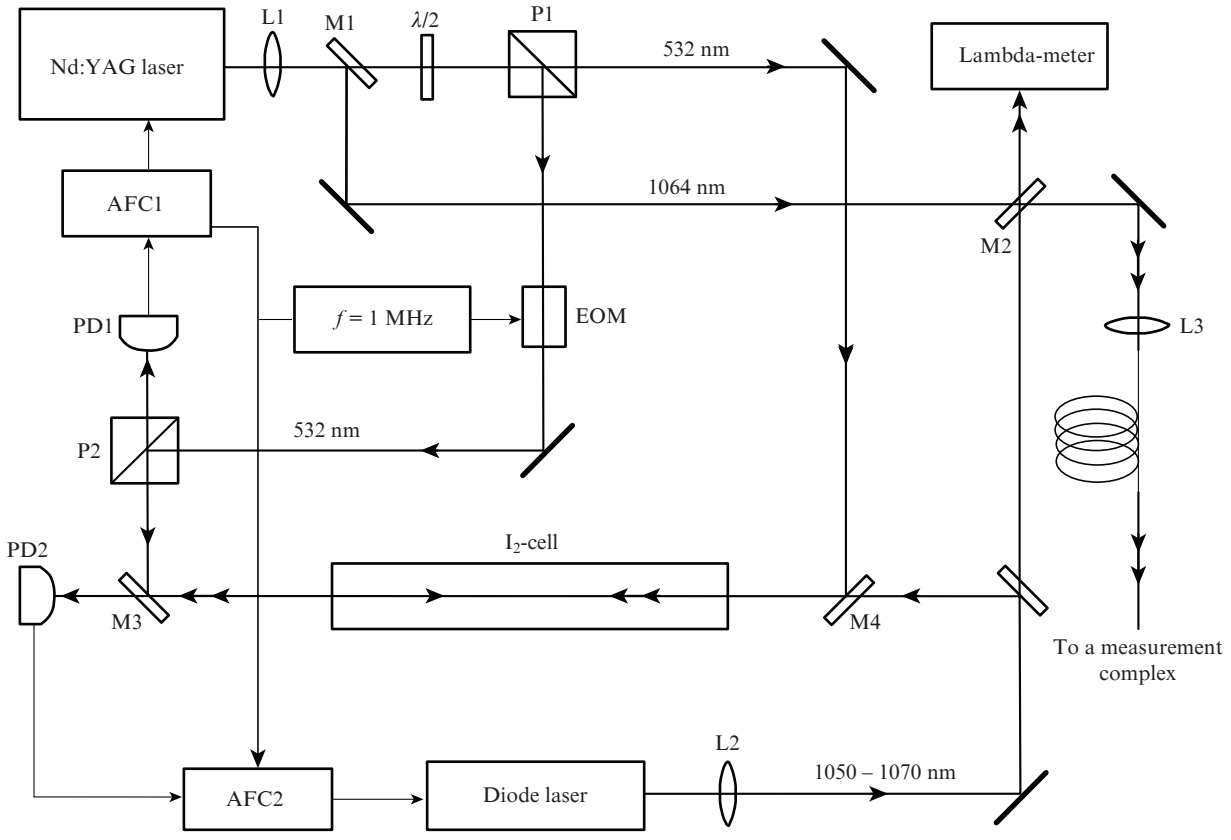

Figure 1. Laser spectrometer for three-level spectroscopy of molecular iodine: (AFC1, AFC2) automatic frequency control systems; (EOM) electro-optical modulator; (PD1) photodiode for the wavelength of 532 nm, (PD2) photodiode for wavelengths 1050–1070 nm; (P1, P2) polarisers; (L1–L3) lenses; (M2) semitransparent mirror; (M1, M3, M4) dichroic mirrors.

The frequency was roughly adjusted within the limits of diode laser gain by turning the outcoupling mirror. Fine adjustment was realised by varying the temperature and exciting current of the laser diode. The operation regime was chosen in such a way that the required frequency of the sounding radiation fit the middle of the instantaneous frequency tuning range. Fine tuning to a prescribed frequency was made by varying the voltage applied to the piezoceramic actuator, on which the diffraction grating was mounted. The instantaneous tuning range without frequency jumps was ~2.5 GHz. The frequency jump boundaries can be shifted by varying the injection current within 2 mA.

In the present work, we used a laser diode with an antireflected output face of the series QLD-1060-50S-AR (QPHOTONICS). The laser provided wavelength tuning in the range of 1050–1070 nm. The output power was 5–7 mW. An elliptical cross section of the output beam was transformed to a circular shape by a pair of anamorphic prisms. Part of the radiation (2–3 mW) was directed to the cell with iodine, and the rest part passed to a precise HighFinesse WS7 wavelength meter.

The glass cell with iodine vapours was 30 cm in length. A vapour pressure in the cell was controlled by varying a temperature of an extension cooled by a Peltier element. A temperature of the extension was stabilised by an electronic control system with an accuracy of 10 mK.

The three laser beams coincided spatially in the iodine cell: the high-intensity saturation radiation of the second-harmonic beam of the Nd:YAG laser, a low-intensity beam of probe radiation at the same frequency, and the sounding beam of the diode laser. The latter two beams were directed towards the saturation beam. By using lenses, the beam configurations were formed in such a way that all the waists were inside the cell. In this case, the diameter of waists for the Nd:YAG-laser beams was 0.5 mm, and for the sounding beam of the diode laser it was 0.4 mm.

The saturation beam changes populations of upper and lower levels in a narrow range of molecule velocity projection onto the beam axis. As a result, a narrow dip arises in the Doppler profile, and a narrow peak arises in the profile of an adjacent emission transition. Since the saturation beam interacts simultaneously with several HFS components of the iodine absorption line, which have overlapping Doppler profiles, the dips and peaks arise in profiles of all the components. A dip on the absorption transition is detected only for the component, for which interaction occurs at the Doppler profile centre where atoms have a zero velocity projection onto the saturation beam axis and, correspondingly, zero Doppler shift. Due to this fact, both the beams (saturation and sounding) interact with the same atoms. Thus, in the case of frequency locking to the frequency of an absorption profile dip, the frequency will exactly equal the transition frequency.

Under tuning the frequency of the sounding laser radiation, the peaks are detected for all the components with which the saturation radiation interacts. In our experiment, the frequency of the sounding laser radiation was locked to the frequency of the peak formed by excited atoms with zero velocity projections. Only in this case the laser radiation frequency exactly equals the emission transition frequency. The condition mentioned above is automatically satisfied at simultaneous locking of the exciting and sounding laser frequencies to the frequencies of iodine line HFS components, corresponding to the transitions with a common upper level. Actually, this condition can be easily satisfied, because hyperfine structures of absorption and emission lines are approximately similar.

Optical resonances were detected by using frequency modulation of the saturation radiation by an electro-optical modulator (EOM) [17]. The modulation frequency was 1 MHz at the modulation index of 0.5. A frequency modulation of the saturation radiation results in modulation of the absorption coefficient on the absorption transition, gain on the emission transition, and, correspondingly, refractive indices at the frequencies of these transitions. As a result, the probe and sounding radiation, having passed through the cell with iodine are modulated both in amplitude and phase. The probe radiation after the cell is detected by a FD265 silicon photodiode, and the sounding radiation is detected by a DFD2000TO InGaAs-pin-photodiode. Signals from the photodiodes pass to phase detectors. Resonances obtained in the result of detection have a dispersion form and are used as error signals for stabilising the radiation frequencies of both lasers by automatic frequency control (AFC) systems.

AFC systems of both lasers have two control loops each: fast and slow. The fast loop provides processing of high-frequency perturbations; the slow loop operates with low-frequency perturbations and slow frequency variations arising under an action of temperature and pressure variations in ambient space. The fast control in the diode laser is realised by changing the injection current, whereas the slow control is made by the piezoceramic on which the diffraction grating is mounted. The frequency of the Nd:YAG-laser radiation is tuned by two piezoceramic elements, on which the cavity mirrors are arranged. One piezoceramic element controls perturbations in the band of up to 5 kHz, and the second element operates in the band of up to 30 kHz.

Diode laser radiation locked to the frequency to a chosen iodine HFS component is directed to a frequency-measurement complex through a fibre-optic cable of length 20 m. In a three-level spectrometer, the radiation frequency stability and absolute value of the sounding laser frequency locked to the frequency of emission resonance depend on the frequency of the pump laser radiation. Our setup was able to control the pump radiation frequency and measure its absolute value. For this purpose, a long-wavelength component of output radiation of the pump Nd:YAG laser was selected by a dichroic mirror M1 and aligned on mirror M2 with the radiation of the diode laser; the combined radiation passed into a fibre-optic cable.

A detailed description of the frequency-measurement complex for absolute frequency measurements is given in [7]. A principal part of the complex is a synthesiser of equidistant optical frequencies based on a femtosecond Ti:sapphire laser with the pulse repetition rate of ~495 MHz. The frequency supercontinuum generated by the laser is then expanded by using a microstructured optical fibre (Femtowhite800). As a result, a supercontinuum occupying the spectral range of 500–1100 nm is generated. In the present work, in contrast to [7] we needed no microstructured fibre, because in the supercontinuum generated in the range 1053–1068 nm the frequency components were sufficiently intense for taking measurements.

In the synthesiser, the mode separation frequency of a Ti:sapphire laser is stabilised due to phase locking of one of the supercontinuum frequency components to the frequency of the Nd:YAG/I_2 standard and to phase locking of the fre-

quency shift f_0 to the frequency synthesised from the frequency of an RF standard. In the result of such locking, from the known frequency of the Nd:YAG/I_2 standard and the frequency shift one can calculate an exact value of the mode separation frequency. High-precision measurements of the mode separation frequency by using a hydrogen standard were also provided.

An accuracy of the system used is determined by that of employed frequency standards: the Nd:YAG/I_2 standard and hydrogen standard. Prior to measurements, the hydrogen standard was calibrated at the Novosibirsk Centre of Metrology. Later, we organised its correction by using GPS. Reproducibility of the hydrogen frequency standard was 10^{-13}. As a Nd:YAG/I_2 standard we used the last modification of a standard (ILP 1064/532-30/50-2A) developed at the Institute of Laser Physics, Siberian Branch of RAS. The standard is described in more details in [15, 18, 19]. It has the high frequency stability: the standard deviation dispersion for 1 s is $\sim 10^{-13}$, for 6×10^4 s it is about 10^{-15}. Reproducibility of the frequency standard is $\Delta\nu/\nu \approx 3\times10^{-13}$ [18].

Frequency reproducibility of an earlier modification of the Nd:YAG/I_2 standard elaborated at the Institute of Laser Physics was studied at the Institute of Quantum Optics (Germany) by comparing this standard with a Nd:YAG/I_2 standard created at PTB (Germany) [20]. The combined frequency reproducibility of both laser systems was no worse than 1.5 kHz. In addition, absolute frequency measurements were taken for a series of I_2 transitions in the range of 532 nm including the transition R56(32–0)a_1 [21]. A frequency of the standard used in the present work was locked to the frequency of this transition. The value of the transition frequency measured (563259651965.5 kHz) was used as a reference in calculation of the mode separation of the synthesiser. This value differs from the value of 563259651971 ± 9.2 kHz recommended by CIMP [22] for R56(32-0)a_1. As shown in [20], this difference can be explained by different temperatures of the cooled branch of the iodine cell in our standard ($T = -5\,^\circ$C) and in the installation, on which the results recommended by CIMP ($T = -15\,^\circ$C) have been obtained. This temperature difference corresponds to a pressure difference of 12 mTorr, and the frequency shift due to pressure in this range is $\Delta\nu/\Delta p = \pm 555$ Hz mTorr^{-1} [18].

During operation, the frequency reproducibility of the Nd:YAG/I_2-standard was periodically controlled by comparing it with the frequency of a second similar standard. The absolute value of the standard frequency was also measured by the synthesiser. For this purpose, the synthesiser mode separation frequencies were used that were measured by the hydrogen standard. In addition, in each measurement, for calculating the measured frequency both the values of the mode separation frequency obtained by the different methods were used. Comparison of two transition frequencies obtained in this way allows one to control the measurement accuracy, which conventionally is within ±1 kHz.

3. Experiment

Choice of the emission transitions, which frequencies can be measured with our setup are determined by tuning ranges of both lasers. Absorption lines pertaining to the bands $\upsilon' - \upsilon'' =$ (32–0), (33–0), (34–0), (35–0) fit the tuning range of second harmonic of the Nd:YAG laser. Most intensive are lines of the (32–0) and (33–0) bands. From emission transitions starting from levels $\upsilon'' = 32$ and 33, the $\upsilon' - \upsilon'' =$ (32–53), (32–54), and (33–54) bands fit the tuning range of the diode laser. Nevertheless, the emission transitions for the (33–54) band are substantially weaker than for the first two bands; the resulting resonance amplitude in these transitions was insufficient for stable locking of the diode laser frequency. Thus, (32–53) and (32–54) bands were chosen for measurements. In each band, three lines with different rotational numbers were chosen, and three HFS components were considered in each line.

Table 1 presents the absorption lines used for pumping and the emission lines corresponding to the transitions, which have a common vibration–rotational level with the transition responsible for the appropriate pumping line. Absorption coefficients for the pump radiation in the cell were equal for all the lines chosen.

The diode laser radiation, which passes to the frequency-measurement complex through an optical fibre cable was mixed with a broadened-spectrum radiation of the Ti:sapphire laser. Then, beatings of diode laser radiation with frequency components of supercontinuum were detected by a fast photodetector. An RF bandpass filter selected the lowest-frequency signal, which was then heterodyned, amplified, and passed to a frequency meter.

Frequency characteristics of the pump laser were studied by direct comparison of its frequency with that of the Nd:YAG/I_2 standard comprised in the frequency-measurement complex. The frequency of pump laser radiation was stabilised by the saturated absorption resonance on the same transition as the frequency of the Nd:YAG/I_2 standard. Hence, in order to avoid the zero-beating problem, we measured the frequency of beatings between the radiation of the pump laser and the second Nd:YAG laser comprised in the Nd:YAG/I_2 standard. The radiation frequency of the Nd:YAG laser was locked to the frequency of the standard by a phase automatic control system with the frequency shift by 40 MHz. The beating signal obtained passed to a frequency meter.

The frequency was measured with intervals of 1 s for time intervals from 10 to 40–50 min. An average frequency value and rms deviation were determined from measurement results. In a measurement session, an rms deviation was within 2–8 kHz. Data obtained were used for plotting Allan variance. In Fig. 2, one can see Allan variance for radiations of the diode laser and pump laser. The pump laser was stabilised by the saturated absorption resonance on the R56(32–0)a_1 transition, whereas the diode laser was stabilised by the emis-

Table 1. Absorption lines and emission transitions used in measurements.

Pump line			Emission line					
Band (32–0)			Band (32–53)			Band (32–54)		
	ν/cm^{-1}	λ/nm		ν/cm^{-1}	λ/nm		ν/cm^{-1}	λ/nm
P54	18786.7726	532.29	P54	9487.543	1054.01	P54	9360.580	1068.31
R56	18788.3427	532.24	R56	9490.884	1053.64	R56	9363.981	1067.92
R60	18781.4413	532.44	R60	9487.722	1053.99	R60	9360.926	1068.27

sion resonance, corresponding to the R56(32–54)a_1 transition. The Allan variances presented, which characterise the beat frequency instability, are mainly related to the radiation frequency instabilities of only the diode and pump lasers, because the frequency instabilities of the Ti:sapphire laser and Nd:YAG/I_2 standard are less than the beating instability by a factor of above an order in magnitude [18].

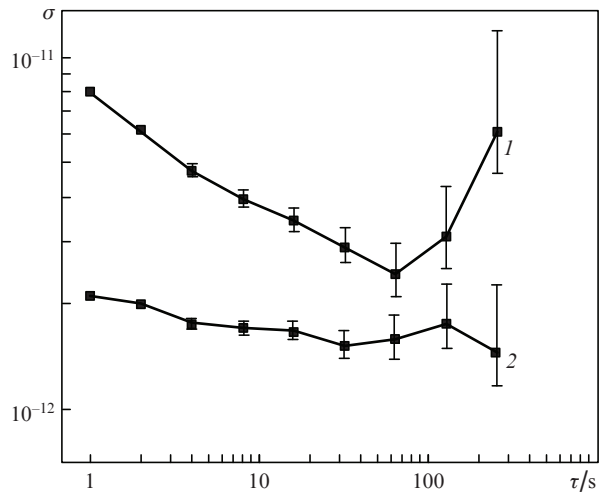

Figure 2. Allan variance for radiation frequencies of (*1*) diode and (*2*) pump lasers.

From measurement results on the beating frequency for the pump laser and Nd:YAG/I_2 standard we determined the absolute value of the pump laser frequency. The shift of the latter relative to the reference frequency was 24.1 ± 1.1 kHz. Note that there is one more frequency shift due to different pressures of iodine in the cell of our setup and in a cell of the frequency standard. The temperature of the cold branch in cell, at which the measurements were taken, maintained equal to 8 ± 0.1 °C. This temperature corresponds to the iodine vapour pressure of 68 mTorr, whereas in the frequency standard the pressure in cell corresponds to a temperature of −5 °C and equals to 18 mTorr. In order to determine the frequency shift due to the pressure difference, we measured the frequency shift of the pump laser as a function of iodine vapour pressure. In the range of 40–87 mTorr, the measured shift coefficient was –375 ± 40 Hz $mTorr^{-1}$.

In Fig. 3, the dependence obtained along with its approximation is presented. One can see that due to the pressure difference, the pump laser radiation frequency should be negatively shifted by 19 ± 2 kHz relative to the reference standard frequency, that is, the real frequency shift is greater than the measured shift by this value and equals 43 ± 2 kHz. The shift due to influence of the sounding radiation of the diode laser tuned to the adjacent transition was also measured. For this purpose, the beat frequency was recorded with and without the sounding radiation. Presence of the sounding radiation in the cell resulted in a noticeable negative frequency jump. In each of the states, beatings were averaged over ~300 s. The value of the shift averaged over four such measurements was 4 ± 0.92 kHz.

Reproducibility of the measurement results was tested in multiple measurements for each of the frequencies. Over the period of four months, 16 measurement series have been performed. In this case, each of the frequencies was measured at

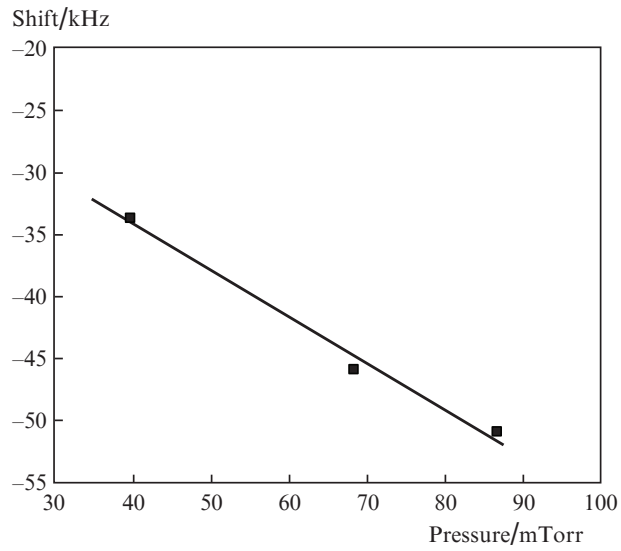

Figure 3. Frequency shift of pump laser radiation vs. iodine vapour pressure in the cell.

least four times. For some transitions with a large data spread, measurements were multiply repeated (up to 8–10 times). Results of five series measured for several days for the component R56(32–53)a_1 are shown in Fig. 4. Each series in the figure is the result of averaging over approximately 1500 values of the beat frequency, each value was obtained by using a frequency meter with the counting time of 1 s.

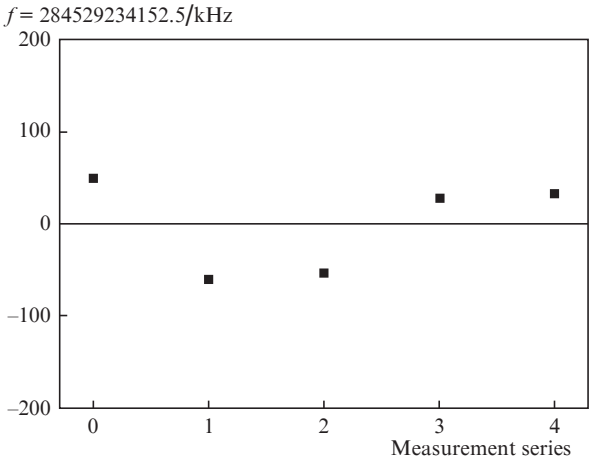

Figure 4. Spread of frequency measurement results for the R56(32–53) a1 component in measurement series.

All measurements were taken at a temperature of the cell cold branch 8 °C. A power of the pump radiation at the cell input was within the limits of 1–3 mW, radiation power of the diode laser at cell input was 0.5–1 mW.

For each iodine transition, the resulting frequency was determined as an average of separate measurement results. The data obtained are given in Table 2. Digits in brackets are rms deviations for measurement results, which exceed the rms deviations of results in a single series by more than an order in magnitude. This circumstance testifies the existence of hardly

Table 2. Frequency measurement results for iodine emission transitions.

Band	Line	Component	Transition frequency /kHz
(32–53)	P54	a_1	284 429 077 823 (53)
		a_{10}	284 429 591 515 (90)
		a_{15}	284 429 849 150 (58)
	R56	a_1	284 529 234 167 (40)
		a_{10}	284 529 747 885 (42)
		a_{15}	284 530 005 268 (50)
	R60	a_1	284 434 462 269 (2)
		a_{10}	284 434 975 997 (50)
		a_{15}	284 435 233 244 (41)
(32–54)	P54	a_1	280 623 120 447 (158)
		a_{10}	280 623 630 250 (14)
		a_{15}	280 623 885 830 (28)
	R56	a_1	280 724 800 547 (154)
		a_{10}	280 725 310 791(146)
		a_{15}	280 725 566 005 (120)
	R60	a_1	280 633 244 603 (235)
		a_{10}	280 633 754 285 (37)
		a_{15}	280 634 009 710 (10)

controllable factors affecting the accuracy of laser frequency locking to the frequency of studied transition. If we assume that the accuracy of our measurements is determined by the worst result then a relative error of obtained frequencies should be 8×10^{-10}. A comparison of the measured frequencies with the values calculated from spectroscopic parameters is not correct, because the measured values correspond to separate lines of transitions between iodine HFS components, whereas the calculated values correspond to a centre of the line presenting a combination of Doppler line profiles for all transitions between HFS components.

In the present work, we employed the experimental setup developed previously, which was intended for demonstrating principal possibilities of the method suggested for absolute measuring iodine emission transition frequencies. We planned to update this setup for improving reproducibility of measurement results; however, in the frameworks of the present work we did not manage to realise all supposed refinements. Nevertheless, we decided to publish the results obtained with a hope that it will be of real interest because the accuracy of data obtained substantially (by tow orders of magnitude) exceeds that of modern experimental data for the transitions considered [13].

4. Discussion of results

Inaccuracy of emission transition frequency measurement in the experiments performed may be related to the error of diode laser radiation frequency locking to the emission resonance centre and error of locking the pump laser radiation frequency to the absorption transition frequency. In a three-level spectrometer, the dependence of the emission resonance frequency on the pump radiation frequency is determined by the relationship [5]:

$$\omega^{\pm} = \omega_{em} \pm (\omega_p - \omega_a)\omega_{em}/\omega_a. \quad (1)$$

Here, ω^+ and ω^- are the centre emission resonance frequencies for unidirectional and counterpropagating beams of the pump and sounding radiations, respectively; ω_{em} and ω_a are the frequencies of emission and absorption transitions, respectively; and ω_p is the pump radiation frequency. From the above relationships we obtain

$$\Delta\omega^+ = \Delta\omega_p\omega_{em}/\omega_a \text{ and } \Delta\omega^- = -\Delta\omega_p\omega_{em}/\omega_a, \quad (2)$$

where $\Delta\omega^+ = \omega^+ - \omega_{em}$ and $\Delta\omega^- = \omega^- - \omega_{em}$ are the frequency shifts of emission resonances from the centre of the emission transition; and $\Delta\omega_p = \omega_p - \omega_a$ is the frequency shift of the pump radiation from the centre of the absorption transition. From relationship (2) one can see that in the conditions of the present experiment, the frequency shift for emission resonance is approximately half the pump radiation frequency shift. In the case of unidirectional beam propagation, the directions of the frequency shifts coincide, whereas for the counterpropagating beams these are opposite.

The factors affecting reproducibility of the radiation frequency of a Nd:YAG laser stabilised by the saturated absorption resonance are well studied and the methods are suggested for minimising this influence [23–25]. In the case of phase modulation used for obtaining the error signal, the most contribution to worsening the accuracy of frequency locking is made by parasitic amplitude modulation of the probe radiation power. This entails appearance of a signal at the modulation frequency, whose value actually does not change when the laser radiation frequency is tuned. This results in a constant signal component at phase detection. A useful signal employed as the error signal has the form of a dispersion curve, the zero point of which corresponds to the transition frequency. In the stabilisation regime, the laser radiation frequency is locked to the zero-signal point. Without constant component, such a point is the transition frequency. A constant component shifts the point and, correspondingly, the locking frequency, which entails a shift of laser frequency locking relative to the transition frequency.

Amplitude modulation of the pump radiation power also leads to modulation of the emission resonance intensity. In the result, after phase detection, the error signal used for locking the diode laser radiation frequency to the resonance frequency acquires a constant component. Correspondingly, the laser frequency shifts relative to the resonance centre.

A value of the shift due to amplitude modulation depends on the slope of the discrimination curve and on the value of the signal constant component. In turn, the slope depends on the resonance width and amplitude. These factors explain noticeably worse frequency reproducibility for the (32–54) band as compared to the (32–53) band. The Franck–Condon coefficient of the (32–53) band is six times greater than that of the (32–54) band; therefore, the resonance amplitude is greater. In the frequency stabilisation regime, the ratio of the error signal to the noise level was 30–50 in the first case and 12–15 in the second case.

One more reason for amplitude modulation arising in the experiment conducted is absorption of the pump radiation by neighbouring HFS components. Lower frequency reproducibility for the component a_1 can be explained by this factor. The range of the pump power action to this component corresponds to the sharpest edge of the sum absorption Doppler profile. As a result, the amplitude modulation for a_1 takes the maximum at a lower resonance amplitude. Amplitude modu-

lation may also occur simultaneously with phase modulation in an electro-optical modulator.

A value of parasitic modulation can hardly be controlled, because it depends on a number of difficult-to-control factors [26]. Presently, the unfavourable effect of amplitude modulation is conventionally suppressed by employing the double-modulation method. A frequency of the probe radiation is modulated at a high frequency (1–10 MHz), whereas the power of pump radiation is modulated by an interrupter at a low frequency (10–50 kHz). High-frequency phase detection selects the discrimination signal, and synchronous detection of this signal suppresses the signal of amplitude modulation. In addition, synchronous detection increases the ratio of the error signal to the noise level.

Thus, an experimental setup with double modulation should comprise a modulator of the pump power. In addition, each spectrometer should include an electro-optical modulator, phase and synchronous detectors, and system of automatic frequency control. Conventionally, in works on stabilising the frequency of Nd:YAG-laser radiation, the pump radiation power is modulated by using an acousto-optical modulator. Such a method for pump power modulation is not suitable for our experiment because an acousto-optical modulator shifts the radiation frequency of the pump laser, and locking to the absorption transition occurs with the shift equal to half the frequency shift of laser radiation. As a result, emission resonances will be excited not at the frequency of the emission transition, but with a shift, the value of which is indefinite because it depends on the emission transition frequency.

We have experimentally verified the method for obtaining optical resonances on absorption and emission transitions by using frequency phase modulation of probe radiations. Here, the pump radiation was not modulated. Intensities of the resonances and, correspondingly, the signal-to-noise ratio increased in this case by several times. An additional increase of the signal-to-noise ratio can be attained due to narrowing the spectral width of diode laser radiation by stabilising the frequency of the latter with a Fabry–Perot interferometer. According to our estimates, realisation of the methods considered will increase the accuracy and reproducibility of measurement results by an order of magnitude.

5. Conclusions

In the present work we have demonstrated the possibility of employing the frequencies of emission transitions between iodine HFS components as standard frequency references for stabilising a laser radiation frequency. A frequency of the diode laser operated in the range of 1050–1070 nm was locked to HFS components of emission lines. The frequency stability at the level of 10^{-11} was obtained for the averaging time of 1 s. For the first time, high-precision frequency measurements were made for certain HFS components of $^{127}I_2$ emission lines in the range of 1053–1068 nm corresponding to the B–X system. By using a femtosecond optical frequency synthesiser, frequencies of 18 HFS components of six emission lines corresponding to (32–54) and (32–53) bands have been measured. The measurement accuracy was 8×10^{-10}, which is by two orders greater than the accuracy of presently available experimental data for these transitions [13]. The main factors worsening the measurement accuracy have been analysed, and methods for minimising their influence due to improvement of the experimental setup have been considered. Estimates show that the measurement accuracy can be enhanced by more than an order.

Systematic measurements according to the methods suggested will provide obtaining new more precise experimental data, which may become a basis for determining exact energies of arbitrary vibration states of the iodine X state. Finally, this will provide more precise spectrometric parameters for calculating frequencies of emission transitions and will make emission spectrum, along with the absorption one, suitable for calibrating laser radiation wavelengths expanding the scale of wavelength references to almost 1.4 μm. The range of frequency references suitable for stabilisation of laser radiation frequency will expand. It is of particular importance for the spectral range of 0.9–1.4 μm with scanty references suitable for frequency stabilisation.

References

1. Bodermann B., Knöckel H., Tiemann E. *Eur. Phys. J. D*, **19**, 31 (2002).
2. Knöckel H., Bodermann B., Tiemann E. *Eur. Phys. J. D*, **28**, 199 (2004).
3. Salumbides E.J., Eikema K.S.E., Ubachs W., Hollenstein U., Knöckel H., Tiemann E. *Mol. Phys.*, **104**, 2641 (2006).
4. Salumbides E.J., Eikema K.S.E., Ubachs W., Hollenstein U., Knöckel H., Tiemann E. *Eur. Phys. J. D*, **47**, 171 (2008).
5. Matyugin Yu.A., Okhapkin M.V., Skvortsov M.N., Ignatovich S.M. *Quantum Electron.*, **38**, 755 (2008) [*Kvantovaya Elektron.*, **38**, 755 (2008)].
6. Liao C.-C., Wu K.-Y., Lien Y.-H., Knöckel H., Chui H.-C., Tiemann E., Shy J.-T. *J. Opt. Soc. Am. B*, **27**, 1208 (2010).
7. Matyugin Yu.A., Ignatovich S.M., Kuznetsov S.A., Nesterenko M.I., Okhapkin M.V., Pivtsov V.S., Skvortsov M.N., Bagayev S.N. *Quantum Electron.*, **42**, 250 (2012) [*Kvantovaya Elektron.*, **42**, 250 (2012)].
8. Yang T., Meng F., Zhao Y., Peng Y., Li Y., Cao J., Gao C., Fang Z., Zang E. *Appl. Phys. B*, **106**, 613 (2012).
9. Hsiao Y.-C., Kao C.-Y., Chen H.-C., Chen S.-E., Peng J.-L., Wang L.-B. *J. Opt. Soc. Am. B*, **30**, 328 (2013).
10. Huang Y.-C., Chen H.-C., Chen S.-E., Shy J.-T., Wang L.-B. *Appl. Opt.*, **52**, 1448 (2013).
11. Kobayashi T., Akamatsu D., Hosaka K., Inaba H., Okubo S., Tanabe T., Yasuda M., Onae A., Hong F.-L. *J. Opt. Soc. Am. B*, **33**, 725 (2016).
12. Huang Y.-C., Guan Y.-C., Suen T.-H., Shy J.-T., Wang L.-B. arXiv1710.09533v1 [physics.atom-ph] 26 Oct 2017.
13. Martin F., Bacis R., Churassy S., Verges J. *J. Mol. Spectrosc.*, **116**, 71 (1986).
14. Beterov I.M., Chebotaev V.P. *Progress in Quantum Electronics*, (New York: Pergamon Press, 1974) Vol. 3, Pt 1, p. 1.
15. Okhapkin M.V., Skvortsov M.N., Belkin A.M., Kvashnin N.L., Bagayev S.N. *Opt. Commun.*, **203**, 359 (2002).
16. Permyakova O.I., Yakovlev A.V., Chapovsky P.L. *Quantum Electron.*, **35**, 449 (2005) [*Kvantovaya Elektron.*, **35**, 449 (2005)].
17. Shirley J.H. *Opt. Lett.*, **7**, 537 (1982).
18. Skvortsov M.N., Okhapkin M.V., Nevskii A.Yu., Bagayev S.N. *Quantum Electron.*, **34**, 1101 (2004) [*Kvantovaya Elektron.*, **34**, 1101 (2004)].
19. Denisov V.I., Ignatovich S.M., Kvashnin S.M., Skvortsov M.N. *Quantum Electron.*, **46**, 464 (2016) [*Kvantovaya Elektron.*, **46**, 464 (2016)].
20. Nevsky A.Yu., Holzwarth R., Reichert J., Udem Th., Hänsch T.W., von Zanthier J., Walther H., Schnatz H., Riehle F., Pokasov P.V., Skvortsov M.N., Bagayev S.N. *Opt.Commun.*, **192**, 263 (2001).

21. Holzwarth R., Nevsky A.Yu., Zimmermann M., Udem Th., Hänsch T.W., von Zanthier J., Walther H., Knight J.C., Wadsworth W.J., Russel P.St.R., Skvortsov M.N., Bagayev S.N. *Appl. Phys. B*, **73**, 269 (2001).
22. Quinn T.J. *Metrologia*, **40**, 103 (2003).
23. Arie A., Byer R.L. *J. Opt. Soc. Am. B*, **10**, 1990 (1993).
24. Eickhoff M.L., Hall J.L. *IEEE Trans. Instrum. Meas.*, **44**, 155 (1995).
25. Hall J.L., Ma L.-S., Taubman M., Tiemann B., Hong F.-L., Pfister O., Ye J. *IEEE Trans. Instrum. Meas*., **48**, 583 (1999).
26. Wong N.C., Hall J.L. *J. Opt. Soc. Am. B*, **2**, 1527 (1985).